

Rydberg transition emission after multielectron capture in low-energy collisions of Ar^{9+} with He, Ne, and Ar

S. Martin, A. Denis, J. Désesquelles, and Y. Ouerdane

*Laboratoire de Spectrométrie Ionique et Moléculaire, Université Claude Bernard (Lyon I),
Campus de la Doua, 69622 Villeurbanne CEDEX, France*

(Received 24 April 1990; revised manuscript received 10 July 1990)

Cross sections for emission of Rydberg transitions in collisions of Ar^{9+} ions with He, Ne, and Ar atoms have been measured at an impact energy of 180 keV. Transitions from levels $n=6, \dots, 11$ and $l=5, \dots, 9$ following multielectron capture and cascading processes have been observed in fast Ar^{7+} , Ar^{6+} , Ar^{5+} , and Ar^{4+} ions. Emission of recoil ions, attributed to transitions in He II, Ne II–IV, and Ar II–IV give an additional proof of the capture of several electrons by the projectile. Doubly excited Rydberg states, also observed in Ar VIII, are due to a multicapture process. Cross sections for multicapture with stabilization of two electrons in Rydberg states are compared to those determined by coincidence measurements.

INTRODUCTION

During the past few years considerable attention was devoted to the studies of charge transfer between highly charged ions and single- or multielectron targets. Apart from the intrinsic interest, such works are important for fusion and astrophysics plasma research.

At low energy ($v < 1$ a.u.), single-electron capture has been found to be state selective, and the basic mechanisms are now well described in a simple classical barrier model (CBM) where angular momentum l depends on relative energy¹ or in a more intricate theory using a perturbed-stationary-state approximation.² Capture of two and more electrons by collision in a multielectron target becomes more probable when highly charged projectiles are considered. Precise theoretical calculations of the multicapture processes are currently not available due to the complexity of the mechanisms involved. Furthermore, the multiexcited states resulting from these processes are not theoretically well known, and we have no data on radiative and autoionizing decay rates of these states at our disposal. However, it is established that multiexcited Rydberg states are populated by multicapture and can be detected by their radiative decays.^{3,4} The population of multiexcited states is predicted by the CBM, but strong evidence has been provided that the multicapture process can involve electron correlation effects that are not accounted for by any independent-electron models.⁵ Branching ratios between autoionization and radiation depend mainly on the core polarization and the nl quantum numbers of the Rydberg electron. Large-angular-momentum states are metastable with respect to autoionization.^{6,7} Photon spectroscopy of Rydberg transitions can give information on the capture levels and the ion charge states, as shown in a previous work on multicapture $\text{Kr}^{18+} + \text{Kr}$ collisions where substates $(n, l) > (18, 17)$ have been excited in several charge states of the projectile, giving rise to transitions observed between $(n, l) = (18, 17), (17, 16), \dots, (9, 8)$ levels in a long cascade chain.⁸

We report here studies on $\text{Ar}^{9+} + \text{He}$, Ne, and Ar at 180 keV energy using Rydberg-state spectroscopy. In the present experiment doubly excited Rydberg states are directly populated in Ar VIII by a double-capture process and not by a double collision as can be the case for other systems.³ Moreover, emission cross sections for multicapture with two-electron stabilization have been measured.

EXPERIMENTAL SETUP

Incident Ar^{9+} ions were extracted at 20 kV from the electron cyclotron resonance (ECR) ion source of LAGRIPPA facility at Grenoble. The experimental arrangement has been described before^{4,8} so that only a few details are given here. Magnetically analyzed Ar^{8+} or Ar^{9+} beams were sent through a circular collimating aperture ($\phi = 5$ mm) in a collision chamber where the gas pressure was maintained at 5×10^{-5} mbar. The beam currents were typically 6 and 2 μA . Photons originating from $\text{Ar}^{9+} + \text{He}$, Ne, and Ar collisions were observed at 90° to the beam axis and focused into the entrance slit of a 0.6-m Czerny-Turner spectrometer. A 1200-line/mm grating blazed at 3000 Å and an EMI 6256 S photomultiplier (PM) were used in the spectral range 2000–6000 Å. For minimizing the background the photocathode of the PM was cooled at -20°C . At 180 keV the Doppler broadening for an opening angle of $\pm 5^\circ$ amounts to $(\Delta\lambda)/\lambda = 2.6 \times 10^{-4}$, which approximately corresponds to the instrumental linewidth obtained with slits opened at 100 μm . We used 250- μm slits throughout the present experiments.

RESULTS

Typical spectra [full width at half maximum (FWHM) of about 2.5 Å] obtained in $\text{Ar}^{9+} + \text{He}$, Ne, and Ar collisions are displayed in Figs. 1(b), 1(c), and 1(d), respectively, together with the identification of the strongest lines. No lines of Ar IX are observable in the recorded

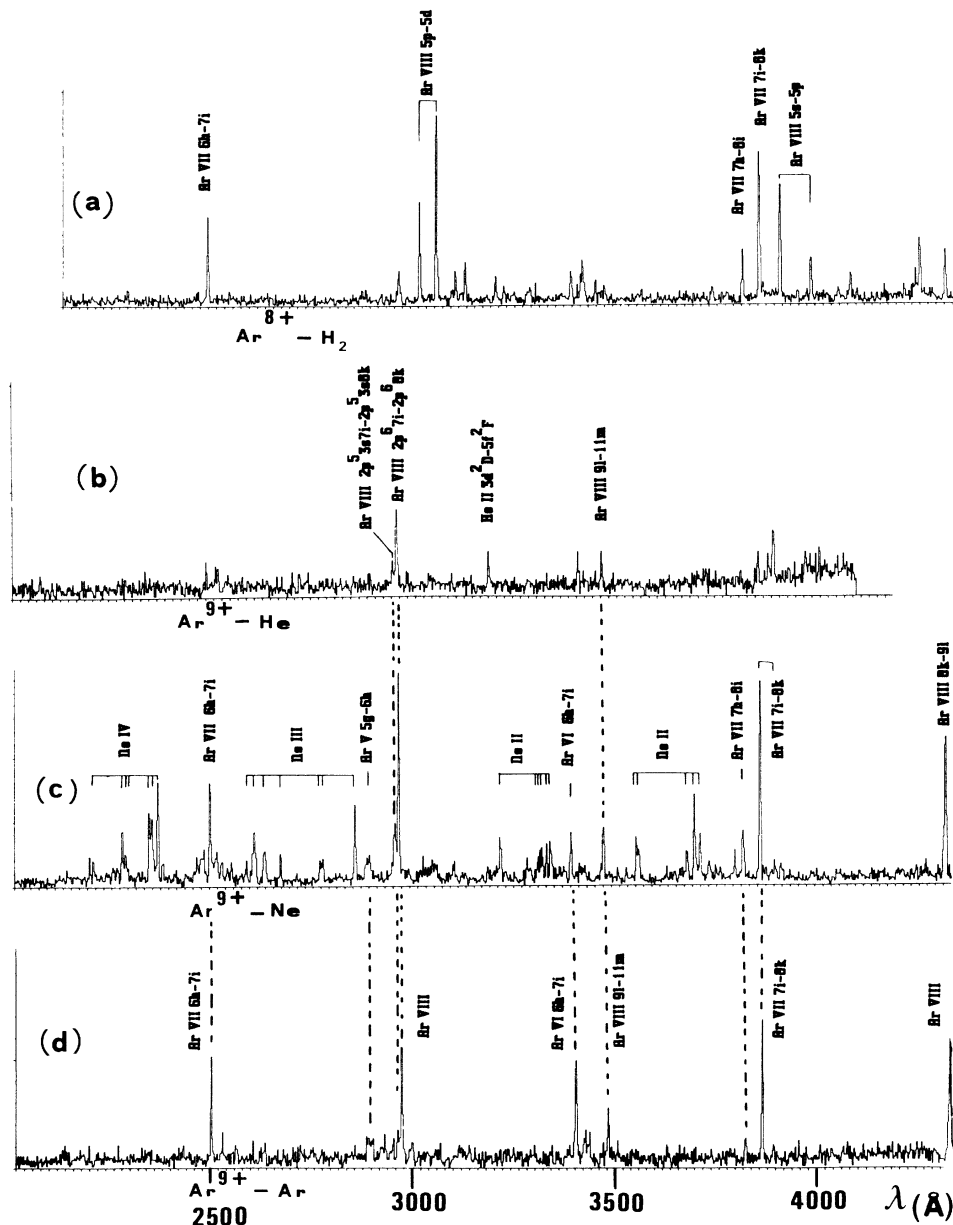


FIG. 1. Spectra from the collisions (a) $\text{Ar}^{8+} + \text{H}_2$, (b) $\text{Ar}^{9+} + \text{He}$, (c) $\text{Ar}^{9+} + \text{Ne}$, and (d) $\text{Ar}^{9+} + \text{Ar}$, from 210 to 440 nm. Lines assigned to Ar VIII, VII, VI, and V refer to Rydberg transitions observed after multielectron capture. He II and Ne II, III, and IV transitions are emitted by recoil ions.

visible region because the $\Delta n = 1$ transitions of Ar IX issued from $n = 5$ and 6, predicted to be populated by single capture, are emitted in the vacuum uv range (Ar IX $n = 4$ to 5 at 500 Å and $n = 5$ to 6 at 920 Å). Therefore only the transitions between Rydberg states due to multicapture may be, and have been, observed in Ar V–VIII from $n = 5, \dots, 11$ levels. The fact that these lines have been produced by multicapture and not by multicollision has been proved by the linearity of the line intensity variations with the gas pressure (Fig. 2). Another evidence for single collision multicapture was demonstrated by the simultaneous observation of highly charged recoil ions.

The absence of charge state impurities, namely Ar^{8+} , in the beam before it ever reached the chamber is demonstrated by the absence of Ar VII lines in the collision with helium. Ar VII lines would be observed as a result of double-electron capture inside the chamber if Ar^{8+} impurities were produced in the upstream residual gas. The intensity weakness of observed transitions $3d \rightarrow 5f$ in He II and $3s \rightarrow 3p$ multiplets in Ne II–IV are in accord with the CBM, which predicts low cross sections for target excitation. He I lines could be seen in the scanned spectral range but were not observed, showing that neutral atoms of the target were not directly excited. The

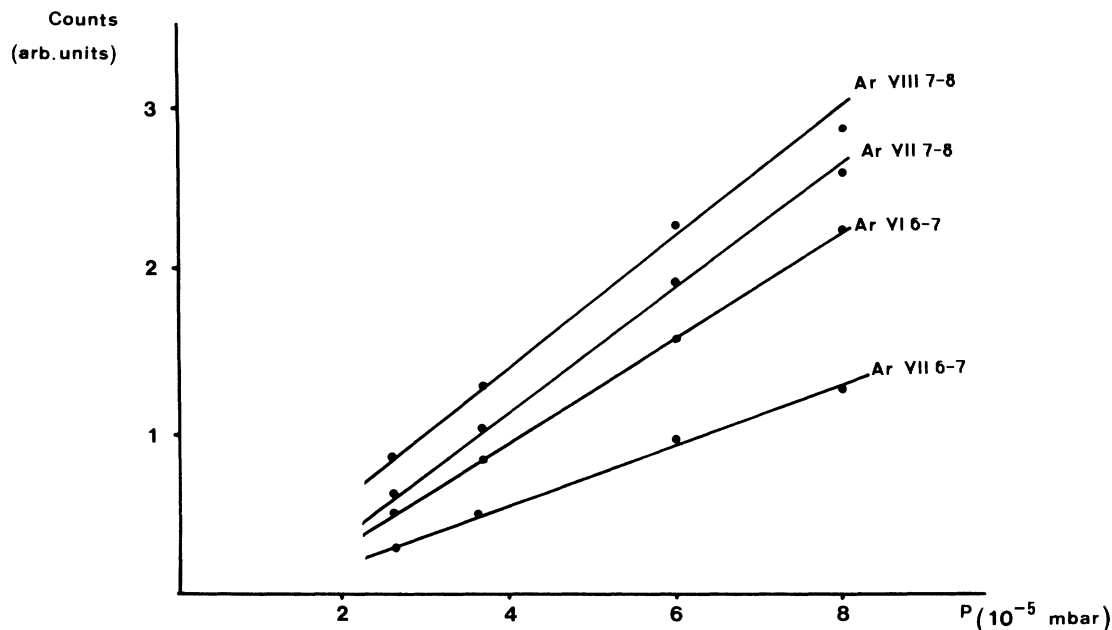


FIG. 2. Pressure variation in intensity of Rydberg transitions emitted after $\text{Ar}^{9+} + \text{Ar}$ collision.

absence of lines from recoil argon ions [Fig. 1(d)] was probably due to the symmetry of the $\text{Ar}^{9+} - \text{Ar}$ collision.

Together with singly excited $2p^6(3s, 3s^2, 3s^2 3p)nl$ configurations, multiexcited configurations can be expected to be produced in collision of Ar^{9+} with the multielectron targets Ne and Ar. In fact core excited Rydberg states $2p^5 3snl$ ($n=6, \dots, 9$) have been observed here in Ar VIII as they have been in a previous experiment where the target was cesium vapor but the excitation processes are different. In $\text{Ar}^{9+} + \text{Cs}$ these states were obtained as a result of two successive processes, a first collision creating Ar^{8+} ($1s^2 2s^2 2p^5 3s^3 P_0$) metastable ions in a proportion of 30–60% and a second one creating Ar^{7+} ($1s^2 2s^2 2p^5 3snl$) doubly excited ions with $n=6, \dots, 11$ and $l=5, \dots, 10$ ⁽³⁾. In the present work the doubly excited Rydberg states have been populated in a single collision by double capture. Single-electron capture from Ar^{8+} impurities, if they existed, would be into the $n=5$ and 6 states of Ar^{7+} and will not explain the observation of $2p^5 3s 9l$ and $2p^6 9l$ configurations. The core excited Rydberg-state population is highly probable as demonstrated by the large intensity of the lines. For example, the Ar VIII $2p^5 3s 7i \rightarrow 2p^5 3s 8k$ transition intensity

amounts to 20% of that of the Ar VIII $2p^6 7i \rightarrow 2p^6 8k$ single excited transition.

Measured wavelengths of Rydberg transitions and recoil ion transitions are listed in Tables I–IV. Lines have been assigned to transitions between the highest angular momenta levels, which is consistent with the weak intensity of $\Delta n=2$ transitions. In fact, the $\Delta n=2$ transitions are necessarily issued from $l \leq n-2$ levels and the $(n, l=n-2) \rightarrow (n-2, l'=n-3)$ and $(n, l=n-2) \rightarrow (n-1, l'=n-3)$ transitions have about the same probabilities. Thus if, for example, the $l=n-2$ states were the only ones populated, the issued $\Delta n=1$ and $\Delta n=2$ transitions would have about the same intensities. A multiconfiguration Dirac-Fock (MCDF) calculation of $2p^6 7l \rightarrow 2p^6 8l'$ transitions shows that Yrast $7i \rightarrow 8k$ and its two nearest $\Delta n=1$ transitions $7h \rightarrow 8i$ and $7g \rightarrow 8h$ could not be resolved in our spectra as their wavelengths are 2976.8, 2976.6, and 2976 Å, respectively. The following component $7f \rightarrow 8g$ is far away (2957 Å MCDF to be compared to 2954 Å from Lindgard *et al.*⁹) and did not appear in Figs. 3(c) and 3(d). Thus from spectra of Ar VIII it is not possible to deduce if the $7h \rightarrow 8i$ and $7g \rightarrow 8h$ components contribute with the $7i \rightarrow 8k$ Yrast to

TABLE I. Transitions of Ar VIII and He II observed in $\text{Ar}^{9+} + \text{He}$ collision.

Transition	λ_{expt} (Å)	λ_{theor} (Å)	σ (10^{-17} cm ²)
Ar VIII $2p^5 3s 7i \rightarrow 2p^5 3s 8k$	2965.8±1		0.06
Ar VIII $2p^6 7i \rightarrow 2p^6 8k$	2975.8±1	2976.8	0.26
He II $3d^2 D \rightarrow 5f^2 F^{\circ}$	3203.1±1	3203.1	0.07
Ar VIII $2p^6 9l \rightarrow 2p^6 11m$	3486.1±1	3488.8	0.07

TABLE II. Transitions of Ar V, Ar VI, Ar VII, and Ar VIII and Ne II, Ne III, and Ne IV observed in Ar⁹⁺ + Ne collision. Prime and double prime give the parent configurations. A detailed description of these transitions in neon can be found in Denis *et al.* (Ref. 10).

Transition	λ (Å)			σ (10 ⁻¹⁷ cm ²)
	This work	(Ref. 10)	Hydrogenic values	
Ne IV 3s ⁴ P → 3p ⁴ P°	2204.3	2203.88		
Ne IV 3s' ² D → 3p' ² F°	2285.4	2285.8		
	2293.4	2293.3		
	2351.1	2352		
Ne IV 3s ⁴ P → 3p ⁴ D°	2358.5	2357		
	2372.5	2372.2		
	2384.5	2384.9		
Ar VII 6h → 7i	2501.6		2523.5	1.98
Ne III 2s ⁵ S → 3p ⁵ P°	2593.0	2590-94-96		
Ne III 3s' ³ D° → 3p' ³ F	2612	2610-13-16		
Ne III 3s'' ³ P° → 3p'' ³ P	2639.2	2639.41		
Ne III 3s ³ S° → 3p ³ P	2678	2678		
Ne III 3s' ³ D° → 3p' ³ D	2777.7	2777.7		
	2785.7	2785.3		
Ne III 3s' ¹ D° → 3p' ¹ F	2866	2866.7		
Ar V 5g → 6h	2904.2		2982.3	0.2
Ar VIII 2p ² 3s7i → 2p ⁵ 3s8k	2965.2			0.4
Ar VIII 2p ⁶ 7i → 2p ⁶ 8k	2975.8		2976.8	1.9
Ne II 3s' ² D → 3p' ² D°	3228.1	3229.5		
Ne II 3s ² P → 3p ² P°	3324.8	3323.7		
Ne II 3s ⁴ P → 3p ⁴ D°	3332.9	3334.9		
Ne II 3s' ² D → 3p' ² P°	3344.9	3344.5		
Ne II 3s ⁴ P → 3p ⁴ D°	3353.0	3355		
Ar VI 6h → 7i	3405.4		3434.8	0.4
Ar VIII 9l → 11m	3486.1		3488.8	0.6
Ne II 3s' ² D → 3p' ² F°	3566.8	3568.5		
	3572.8	3579.6		
Ne II 3s ⁴ P → 3p ⁴ P°	3692.9	3694		
Ne II 3s ² P → 3p ² D°	3712.1	3713		
	3726.2	3727		
Ar VII 7h → 8i	3833.3		3888.1	0.3
Ar VII 7i → 8k	3875.8		3888.1	1.6
Ar VIII 8k → 9l	4340.4		4341.9	1.7

TABLE III. Transitions of Ar V, Ar VI, Ar VII, and Ar VIII observed in Ar⁹⁺ + Ar collision.

Transition	λ (Å)			σ (10 ⁻¹⁷ cm ²)
	This work		Hydrogenic values	
Ar VII 6h → 7i	2501.6		2523.5	1.9
Ar VIII 8k → 10l	2529.6		2531.3	0.3
Ar V 5g → 6h	2904.2		2982.3	0.4
Ar VIII 2p ⁵ 3s7i → 2p ⁵ 3s8k	2965.2			0.3
Ar VIII 2p ⁶ 7i → 2p ⁶ 8k	2975.8		2976.8	1.6
Ar VI 6h → 7i	3405.2		3434.8	1.4
Ar VIII 9l → 11m	3486.9		3488.8	1.0
Ar VII 7h → 8i	3833.1		3888.1	0.3
Ar VII 7i → 8k	3874.6		3888.1	1.6
Ar VIII 8k → 9l	4338.1		4341.9	2.2
Ar VII 9l → 11m	4551.1		4556.8	0.7

TABLE IV. Transitions of Ar VII and VIII observed in $\text{Ar}^{8+} + \text{H}_2$ collision.

Transition	λ (Å)		σ (10^{-17} cm 2)
	This work	Hydrogenic values	
Ar VII $6h \rightarrow 7i$	2501.6	2523.5	0.75
Ar VIII $5p^2P_{1/2} \rightarrow 5d^2D_{3/2}$	3028.9		0.5
Ar VIII $5p^2P_{3/2} \rightarrow 5d^2D_{5/2}$	3069.1		1.26
Ar VII $7h \rightarrow 8i$	3833.3	3888.1	0.2
Ar VII $7i \rightarrow 8k$	3874.6	3888.1	1.2
Ar VIII $5p^2S_{1/2} \rightarrow 5d^2P_{3/2}$	3929		1.0
Ar VIII $5p^2S_{1/2} \rightarrow 5d^2P_{1/2}$	4004		0.3

the intensity of the line observed at 2976 Å. This is also true for the $n = 8$ to 9 transition in Ar VIII. Nevertheless by comparing the Ar VII $7i \rightarrow 8k$ and $7h \rightarrow 8i$ of Figs. 3(a), 3(c), and 3(d) which were resolved due to a larger polarization of the core and were observed with intensity ratios of about 5 and 6, it seems to be more probable that the $(n-1, l-1) \rightarrow (n, l)$ transitions are relatively weak when $l \leq n-2$. Such comments can be made for $2p^5 3snl$ satellites. Measured wavelengths of Rydberg transitions are compared with computed hydrogenic values. Differences are mainly due to the dipole polarization. For the wavelengths of recoil ions, we compare them to beam-foil data.¹⁰

Emission cross sections are reported in the last column of Tables I-IV. They were deduced from line intensities after corrections for spectral response of the detection system. Knowing the emission cross sections of the Ar VIII $5d \rightarrow 3p$ transition in $\text{Ar}^{8+} + \text{H}_2$ (Ref. 11) and using hydrogenic branching ratios,⁹ we were able to deduce the emission cross sections of the $5p^2P_{1/2} \rightarrow 5d^2D_{3/2}$, and

$5p^2P_{3/2} \rightarrow 5d^2D_{5/2}$ transitions in Ar VIII [Fig. 1(a)] and from them the absolute response of our optical system at the corresponding wavelengths. Cross sections for all other lines in all spectra derive from the relative spectral efficiency curve of the spectrometer and photomultiplier. Error bars amount to about 30%. Note that lines assigned to Ar VII $6h \rightarrow 7i$, $7i \rightarrow 8k$, and $7h \rightarrow 8i$ due to double capture are also observed in the $\text{Ar}^{8+} + \text{H}_2$ collision.

DISCUSSION

Measured cross sections for emission of $7i \rightarrow 8k$, $6h \rightarrow 7i$, and $5g \rightarrow 6h$ transitions in Ar V-VIII have been plotted as a function of the Δq exchange charge for the three systems $\text{Ar}^{9+} + \text{He}$, $\text{Ar}^{9+} + \text{Ne}$, and $\text{Ar}^{9+} + \text{Ar}$ in Fig. 3. A net decrease of cross sections for increasing Δq is demonstrated. The emission cross sections for double capture by Ar^{9+} are much weaker in He than in Ne and Ar (in ratios 1:6:5). Coke *et al.*¹² have found in a coincidence experiment for measuring true double capture ($q = 9$ to 7) a ratio of 1:3 for Ar^{9+} in He and Ne. Furthermore measured emission cross sections (0.3×10^{-17} , 1.9×10^{-17} , and 1.6×10^{-17} cm 2) are all largely smaller than cross sections for true double capture (10×10^{-17} and 30×10^{-17} cm 2). True double-capture cross sections have been measured by Coke *et al.* at lower energy but it is known that cross sections for ionization transfer are almost independent of the projectile velocity.¹³ Thus we conclude that we have observed only a part of the true double capture.

Questions on possible processes populating doubly excited states of Ar VIII can claim our attention. The observed line intensities are not only functions of the direct population of the transition upper levels during the collision but also of cascades and branching ratios. Intensities of the lines at 4342 and 2976 Å show the importance of cascades from $n = 9$ to 8 levels in Ar VIII. The quasiequality of the measured intensities demonstrates that the $n = 8$ levels are not much directly populated and that collisions populate mostly levels higher (probably much higher) than $n \approx 8$. For the core excited $3snl$ configurations in Ar VIII, results of Luc-Koenig and Bauche⁷ show that high l ($l = n-1, n-2, n-3$) states mostly decay radiatively. Autoionization is only important for low l states. The CBM predicts that double cap-

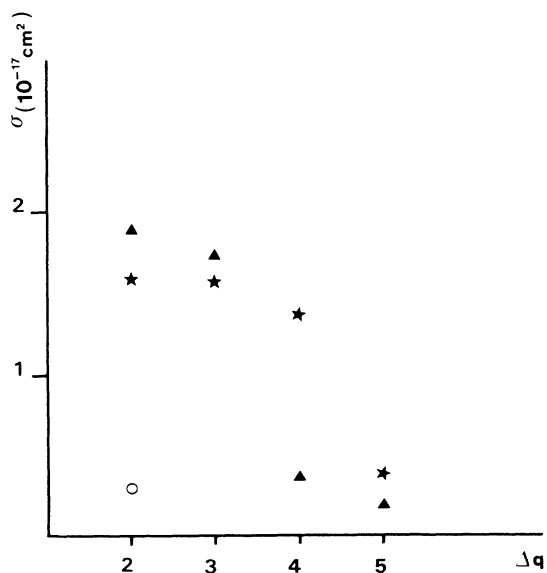


FIG. 3. Plot of emission cross sections vs charge transfer Δq , for \circ , He; \blacktriangle , Ne; \star , Ar. The $7i \rightarrow 8k$ transitions are associated with $\Delta q = 2$ and 3 and the $6h \rightarrow 7i$, $5g \rightarrow 6h$ transitions are related to $\Delta q = 4$ and 5, respectively.

ture in $\text{Ar}^{9+} + \text{Ar}$ collision populates $n=5$, $n'=5$ levels. However, the energy diagram shows that $n=4$, $n'=9$ levels can also be populated, in agreement with present experiment. The observation of light from $1s^2 2s^2 2p^5 3snl$ doubly excited Rydberg states shows that the $n=4$, $n'=9$ levels are not completely autoionizing although the energy of the $n=3$ to 4 inner-shell electron transition does not forbid the autoionization of the Rydberg electron.

Comparisons, similarities and differences, between structures of doubly excited Rydberg states obtained by a double-capture process as in the present experiment or in

a double collision raise interesting questions. We are undertaking further work to clarify these points and to provide more information on these structures.

ACKNOWLEDGMENTS

The authors would like to thank T. Lamy, A. Brenac, and G. Lamboley for their assistance in running the ECR ion source. The Laboratoire de Spectrométrie Ionique et Moléculaire is "Unité associée au Centre National de la Recherche Scientifique No. 171."

¹A. Niehaus, *J. Phys. B* **19**, 2925 (1986).

²C. Harel and A. Salin, *J. Phys. B* **13**, 785 (1983).

³S. Martin, G. Do Cao, A. Salmoun, T. Bouchama, A. Denis, J. André, J. Désesquelles, and M. Druetta, *Phys. Lett. A* **133**, 239 (1988).

⁴S. Martin, A. Salmoun, Y. Ouerdane, M. Druetta, J. Désesquelles, and A. Denis, *Phys. Rev. Lett.* **62**, 2112 (1989).

⁵N. Stolterfoht, C. C. Havener, R. A. Phaneuf, J. K. Swenson, S. M. Shafroth, and F. W. Meyer, *Phys. Rev. Lett.* **57**, 74 (1986).

⁶M. Poirier, *Phys. Rev. A* **38**, 3484 (1988), and private communication.

⁷E. Luc-Koenig and J. Bauche, *J. Phys. B* **23**, 1763 (1990).

⁸S. Martin, A. Denis, Y. Ouerdane, A. Salmoun, A. El Motasadeq, J. Désesquelles, M. Druetta, D. Church, and T. Lamy, *Phys. Rev. Lett.* **64**, 2633 (1990).

⁹A. Lindgard and S. E. Nielsen, *At. Data Nucl. Data Tables* **19**, 6 (1977).

¹⁰A. Denis, J. Désesquelles, and M. Dufay, *J. Opt. Soc. Am.* **59**, 976 (1969).

¹¹M. Druetta, S. Martin, T. Bouchama, C. Harel, and H. Jouin, *Phys. Rev. A* **36**, 3071 (1987).

¹²C. L. Coke, R. Dubois, T. J. Gray, E. Justiniano, and C. Can, *Phys. Rev. Lett.* **46**, 1671 (1981).

¹³E. Salzbom, W. Groh, A. Müller, and A. S. Schlachter, *Phys. Scr.* **T3**, 148 (1983).